

NASA Technical Memorandum 87614

**WAVELENGTH ERROR ANALYSIS IN A MULTIPLE-BEAM FIZEAU
LASER WAVEMETER HAVING A LINEAR DIODE ARRAY READOUT**

D. M. ROBINSON; C. L. FALES, JR.; AND M. W. SKOLAUT, JR.

DECEMBER 1985

FOR REFERENCE

NOT TO BE TAKEN FROM THIS ROOM

LIBRARY COPY

DEC 19 1985

**LANGLEY RESEARCH CENTER
LIBRARY, NASA
HAMPTON, VIRGINIA**



**National Aeronautics and
Space Administration**

**Langley Research Center
Hampton, Virginia 23665**

10 1 1 RN/NASA-TM-87614

DISPLAY 10/2/1

86M16089** ISSUE 6 PAGE 1025 CATEGORY 74 RPT#: NASA-TM-87614 NAS
1:15:87614 85/12/00 46 PAGES UNCLASSIFIED DOCUMENT

UTTL: Wavelength error analysis in a multiple-beam Fizeau laser wavemeter having
a linear diode array readout

AUTH: A/ROBINSON, D. M.; R/FALES, C. L., JR.; C/SKOLAUT, M. W., JR.

CORP: National Aeronautics and Space Administration. Langley Research Center,
Hampton, Va. AVAIL. NTIS

SAP: HC A03/MF A01

COI: UNITED STATES

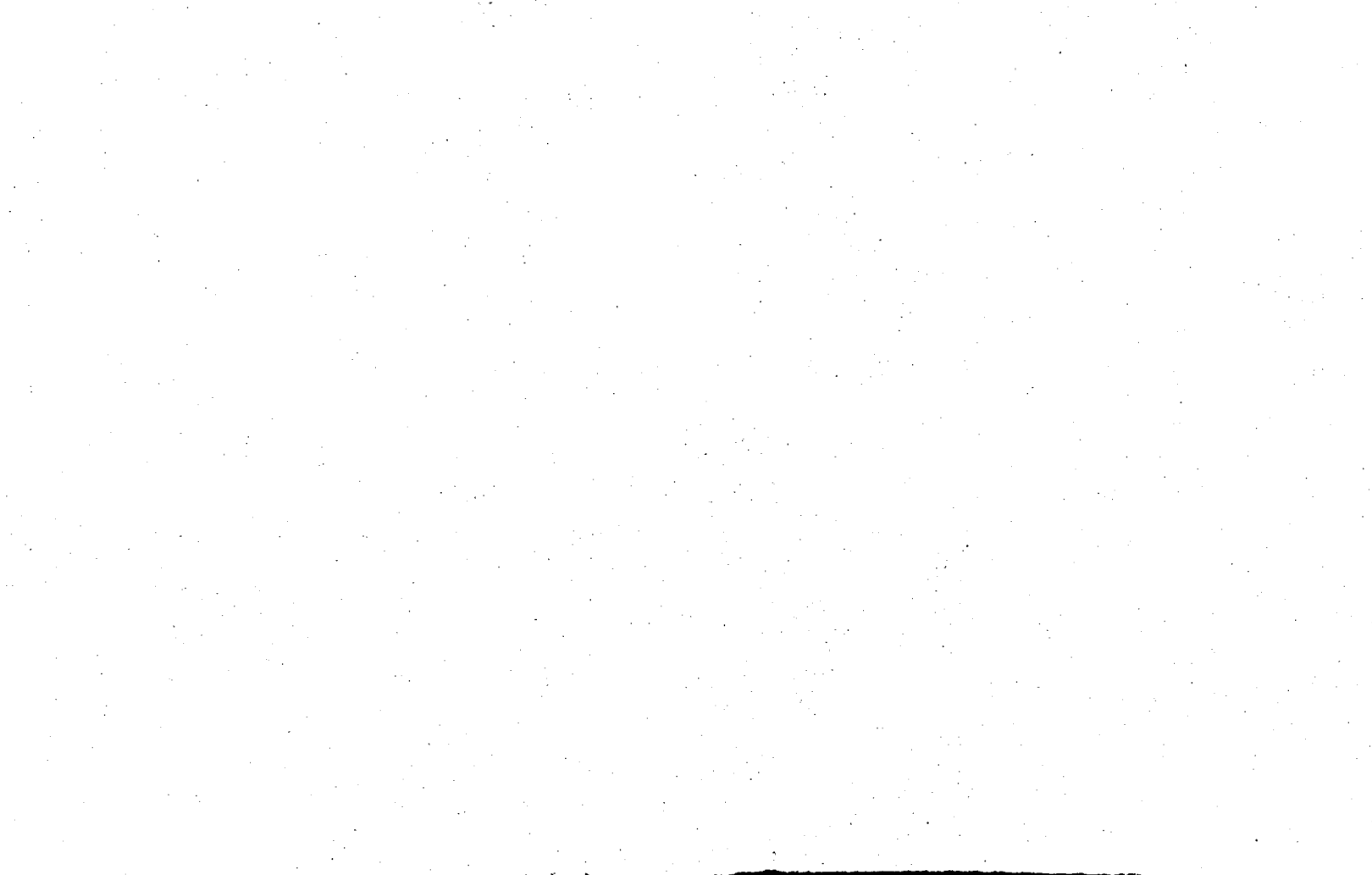
MAJS: /*ARRAYS/*DIFFRACTION PATTERNS/*ERROR ANALYSIS/*FIZEAU EFFECT/*FRINGE
MULTIPLICATION/*INTERFEROMETERS/*LASER DOPPLER VELOCIMETERS/*LIMFAR
SYSTEMS/*PHOTOELECTRICITY/*WAVELENGTHS

MINS: / DIODES/ NOISE SPECTRA/ OPTICAL RADAR/ SPECTROSCOPY/ TUNABLE LASERS

ABA: Author

ABS: An estimate of the wavelength accuracy of a laser wavemeter is performed
for a system consisting of a multiple-beam Fizeau interferometer and a
linear photosensor array readout. The analysis consists of determining the
fringe position errors which result when various noise sources are
included in the fringe forming and detection process. Two methods of
estimating the fringe centers are considered: (1) maximum pixel current
location, and (2) average pixel location for two detectors with nearly
equal output currents. Wavelength error results for these two methods are

ENTER:



List of Symbols

λ	Wavelength
x	Fringe coordinates
m	Fringe order number
$h(x)$	Fizeau wedge height at given location
\bar{X}	Fringe spatial period
β	Fizeau wedge angle
L	Fringe separation
A	Fringe irradiance
P	Optical power in fringe
ρ	Fringe half-width at half-power
$t(x)$	Aperture function of detector element
Δ	Width of detector element
k	Continuous non-integer variable in detector plane
$R(x)$	Detector response function
$r(x)$	Detector response variation about a mean value
$I(x)$	Current output from detector array at location, x .
Q	Current quantization value
σ_n	Current fluctuation due to noise
SNR	Signal-to-Noise Ratio
N	Number of detector elements contained in fringe width
e	Error parameter describing fringe location uncertainty
p	Probability density function
$\delta\lambda$	Spectral width
z	Parameter describing detector element separation

Abstract

An estimate of the wavelength accuracy of a laser wavemeter is performed for a system consisting of a multiple-beam Fizeau interferometer and a linear photosensor array readout. The analysis consists of determining the fringe position errors which result when various noise sources are included in the fringe forming and detection process. Two methods of estimating the fringe centers are considered: 1) maximum pixel current location, and 2) average pixel location for two detectors with nearly equal output currents. Wavelength error results for these two methods are compared for some typical wavemeter parameters.

Introduction

The use of tunable laser sources in fields such as spectroscopy and lidar often require that some method be used to accurately determine the wavelength of the laser. Depending upon the constraints of the particular application factors such as weight, volume and spectral coverage can dictate what types of wavelength measuring devices are suitable to satisfy the experimental requirements. For those applications where space is limited and where both pulsed and cw lasers are used, Fabry-Perot or Fizeau interferometers interfaced with linear diode array sensors are attractive. In this approach, the wavelength is determined by measuring the fringe locations of the various laser sources by the diode array. Since the measured fringes are, in general, distorted by errors introduced in the detection process, the accuracy of this method depends upon how well the position of the measured fringes corresponds to the true fringe positions generated by the interferometer.

N86-16089 #

In this paper, the wavelength accuracy of a Fizeau-type wavemeter having a linear photosensor array readout is presented. The results show that the wavelength errors depend upon both the method used to measure the fringe locations and to errors in the system including: (1) response non-uniformity of the sensor array; (2) current quantization errors; (3) electronic signal-to-noise ratio; and (4) spectral irradiance non-uniformity across the interferometer aperture.

Background

Basically, interferometers are classified into two groups: (1) two-beam interferometers where the fringes can be described according to two-beam interference; (2) multiple-beam interferometers where fringe sharpening is obtained by the interference of multiple beams. A good example of a wavemeter of the first type is one developed by Snyder, et al. (Ref. 1) in which a Fizeau wedge with uncoated plates is used. This low finesse interferometer attains wavelength accuracy through the combined use of selected electronic filtering and computer algorithms to determine the period of interference fringes. An example of a wavemeter of the second type is one employing either a Fabry-Perot (Refs. 2, 3) or Fizeau interferometer (Ref. 4) in which the plates are coated for high reflectivity. This form of wavemeter has much sharper fringes (high finesse) than the two-beam type and consequently can resolve and display complex spectral structure.

The analysis presented in this paper is for an interferometer of the second type. Specifically, the equations are developed for a multiple-beam Fizeau using a standard laser of known wavelength (e.g., frequency stabilized He-Ne) as a reference. However, the procedures used for error determination of the fringe positions may be applied to any measurement device in

which the relative position of known and unknown laser fringes are measured via a linear photosensor array.

Wavelength Measurement Concept

Figure 1 shows the basic geometry of a Fizeau interferometer. In this diagram, the two inner surfaces of the plates are inclined at a wedge angle, β , and the positions of the fringes resulting from illuminating the aperture of the interferometer with spectrally uniform, nearly collimated light of wavelengths, λ_0 (known wavelength), and λ_u (unknown wavelength) are shown at coordinates x_0 , x_u , and x_{0+1} . These coordinates correspond to the fringe orders m_0 , m_u , and m_{0+1} and wedge heights of h_0 , h_u , and h_{0+1} . If we assume that the medium separating the two surfaces is evacuated (index = 1) then the period of the unknown and known fringes is given by $X_u = \lambda_u/2\beta$ and $X_0 = \lambda_0/2\beta$. If the separation of the unknown fringe of order, m_u , relative to the known fringe of order, m_0 , is given by $L = x_u - x_0$, then it is easy to show that the relationship between these fringes is

$$m_u \lambda_u = (m_0 + L/X_0) \lambda_0 \quad (1)$$

As can be seen from fig. 1, the detected fringes, whose peaks are located at the stated coordinates, possess finite widths due to the quasi-monochromatic nature of the laser sources and also due to the fringe broadening effects of the interferometer (i.e., the instrument finesse). Further, since these fringes have been distorted by errors in the detection process (e.g., non-uniformity of photosensor response, etc.), the accuracy with which the wavelength can be determined depends upon the values of L and X_0 of the distorted fringes relative to the values which would be

obtained if the detection process were perfect. Taking differentials of both sides of eq. (1) and assuming that m_0 can be determined exactly by calibration procedures with the known laser, one may determine the relative uncertainty in the order, m_u , to be

$$\frac{\Delta m_u}{m_u} = \frac{1}{m_0} \left(\frac{\Delta L}{X_0} + \frac{L}{X_0} \cdot \frac{\Delta X_0}{X_0} \right) + \frac{\Delta \lambda_0}{\lambda_0} + \frac{\Delta \lambda_u}{\lambda_u} \quad (2)$$

where we have taken only plus signs as a worst case value. If from other means (e.g., a pre-monochrometer, etc.) the order, m_u , can be determined such that its uncertainty is $m_u < 0.5$, and assuming $\Delta \lambda_0 / \lambda_0 \ll \Delta \lambda_u / \lambda_u$, then an upper bound on the relative wavelength uncertainty is given by

$$\left| \frac{\Delta \lambda_u}{\lambda_u} \right| \leq \frac{1}{m_0 X_0} \left(|\Delta L| + |L \Delta X_0| \right). \quad (3)$$

From the definitions of L and X_0 the accuracy of this wavelength determination depends upon the errors obtained in measuring the various coordinate locations of the fringes.

Estimate of Linecenter by Peak Location

For a given set of spectral lines, or fringes, which have been detected and stored for processing, several methods can be used to measure their positions. The particular approach chosen depends upon several factors. These include the wavelength accuracy required, any a priori knowledge of

the fringe shape, and the time allowed for processing the measurement data. One method for this measurement in a system with a diode array readout is by peak location. In this approach it is assumed that the peak of the fringe irradiance incident upon a perfect array generates the maximum signal current. Thus, the determination of the diode location having the maximum current locates the peak. As will be shown, however, noise in the detection process leads to current fluctuations which distort the true shape of the fringe and consequently the peak location.

Error Analysis

The error analysis of this method begins with reference to fig. 2 which illustrates the fringe irradiance incident on the array. In this figure we have neglected the slight asymmetric fringe shape and "ringing" that is characteristic of the multiple-beam Fizeau (Ref. 5) and have assumed the fringe shape to be Lorentzian, i.e., having the same shape as Fabry-Perot fringes (Ref. 6). Consequently, we can write the irradiance of a single fringe as

$$A(x) = \frac{P_0/\pi\rho}{1 + \left(\frac{x-x_0}{\rho}\right)^2} \quad (4)$$

where P_0 is the optical power contained in the fringe incident on the detector plane at $x = x_0$ and 2ρ is the full-width-half-max (FWHM) of the fringe.

If a sensor element of width, Δ , is located with its center at x_d , and has an aperture function given by $t(x) = \text{Rect} [(x-x_d)/\Delta]$, the optical power incident upon the element is the convolution

$$P(x_d) = \int_{-\infty}^{\infty} \frac{P_0/\pi\rho}{1 + (x/\rho)^2} \text{Rect} \left[\frac{x - (x_d-x_0)}{\Delta} \right] dx. \quad (5)$$

Let us assume that x_0 is located within some particular sensor element whose center is defined as the center of our coordinate system (i.e., $|x_0| \leq 0.5$). Further, let us replace the variable, x , in eq. (5) by $x = k\Delta$ where k is continuous and has values at the centers of the sensor elements of $k_d = 0, \pm 1, \pm 2, \dots$. Using these conditions and defining a diode response function, $R_d(k\Delta)$, whose value depends upon the coordinate, $k\Delta$, then the current output from the array is

$$\begin{aligned} I(k\Delta) &= R_d(k\Delta) \int_{(k-x_0/\Delta - 1/2)\Delta}^{(k-x_0/\Delta + 1/2)\Delta} \frac{d\xi/\rho}{1 + (\xi/\rho)^2} \\ &= R_d(k\Delta) \left(\frac{P_0}{\pi} \right) \left\{ \tan^{-1}[(k-x_0/\Delta + 1/2) \Delta/\rho] - \tan^{-1}[(k-x_0/\Delta - 1/2) \Delta/\rho] \right\}. \end{aligned} \quad (6)$$

The values at $k_d = 0, \pm 1, \pm 2$, give the current from the various detector elements.

If we further define the array response function to be $R_d(k\Delta) = R_0 + r(k\Delta)$ where R_0 is the response at $k\Delta = 0$ and $r(k\Delta)$ is the variation of

the response about this value, then equation (6) can be expressed as

$$I(k\Delta) = (I_0/\theta_0) \left[1 + \frac{r(k\Delta)}{R_0} \right] \tan^{-1} \left\{ \frac{\Delta/\rho}{1 + [(k-x_0/\Delta)^2 - 1/4](\Delta/\rho)^2} \right\}. \quad (7)$$

In this equation, $\theta_0 = 2\tan^{-1}(\Delta/2\rho)$ and the current, I_0 , is the current obtained when k and x_0 are zero and $R_d = R_0$ (i.e., $I_0 = (R_0 P_0 \theta_0)/\pi$).

For a perfect array with uniform response, a plot of output current from the array for different values of the parameter, $|x_0|/\Delta$, is shown in fig. 3. Note that for $|x_0|/\Delta = 0.5$, the peak current is the same on adjacent elements so that the actual location of the peak is uncertain to $\pm 0.5\Delta$.

The function, $R_d(k\Delta)$, present in eq. (7) accounts for those current fluctuations which are due to response non-uniformities of the diode array. This function can also be used to account for errors which are introduced into the measurement by non-uniform spectral irradiance across the Fizeau aperture.

If a small noise modulation is added to the irradiance function given by eq. (4) the corresponding optical power incident on a single diode is obtained by modifying eq. (5) to include a small power fluctuation, P_n . The diode array output current is then

$$I'(k\Delta) = P(k\Delta) \left[R_0 + r(k\Delta) + R_0 \cdot \frac{P_n}{P} + r \cdot \frac{P_n}{P} \right]. \quad (8)$$

If the last term in this equation is small then the current is

$$I'(k\Delta) \approx P(k\Delta) \left[R_0 + r(k\Delta) + r_n(k\Delta) \right] \quad (9)$$

where $r_n = R_0(P_n/P)$ is the effective response variation in the array due to the non-uniform illumination. If we define a total response variation, $r_t = r + r_n$, and let $R = r_t/R_0$, the previous equation becomes

$$I'(k\Delta) \approx P(k\Delta) R_0 \left[1 + R \right]. \quad (10)$$

In addition to the current fluctuations just described, other fluctuations are present in the form of current quantization errors and signal-to-noise considerations. Specifically, if the maximum signal current from the diode array is digitized into Q current intervals of $\Delta I = I_0/Q$, then a current error of $\Delta I_q = \pm \Delta I/2$ is present in the detection process as well as a current fluctuation of $\pm \sigma_n$ if signal-to-noise effects are included. Thus, the signal currents shown in fig. 3 for uniform response and no noise must be modified. This results in a peak location uncertainty which is greater than our previous result of $\pm 0.5\Delta$. Referring to fig. 4, it is easy to see that a worst-case combination of these error sources results in an uncertainty of the signal peak given by the relation

$$I' \left[k\Delta=0; r_t(k\Delta) = -r_t \right] - \sigma_n - \Delta I/2 = I' \left[k\Delta; r_t(k\Delta) = +r_t \right] + \sigma_n + \Delta I/2 \quad (11)$$

where $I'(k\Delta; r_t)$ is given by eq. (7) with r replaced by r_t . Solving this expression for $k\Delta$ gives the coordinate location which satisfies eq. (11). The corresponding value of k is

$$k = \bar{x} \pm 1/2 \quad X$$

$$\sqrt{1+N^2 \left\{ \frac{2/N}{\tan \left\{ \frac{(1-R)}{(1+R)} \tan^{-1} \left(\frac{2/N}{1+[\bar{x}^2-1/4](2/N)^2} \right) - \frac{\theta_0 [2(\text{SNR})^{-1}+Q^{-1}]}{1+R} \right\}} - 1 \right\}} \quad (12)$$

where we have defined the parameters $\bar{x} = x_0/\Delta$, $\text{SNR} = I_0/\sigma_n$, and $N = 2\rho/\Delta$ is the number of diodes that are contained in the fringe width, 2ρ . Since the diode centers are located at integer multiples of Δ , the value obtained in eq. (12) is reduced to the integer which satisfies $k_d < |k|$.

From the integer obtained above, reference to fig. 4 shows that the absolute error, $|\Delta x_i|$, in locating the peak of a particular fringe at coordinate, x_i , is given by $|\Delta x_i| = |k_d\Delta - x_0|$. However, since the location of x_0 within the $k_d = 0$ diode is unknown to within $\pm \Delta/2$, the value of x_0 must be varied within these limits such that the difference $|k_d\Delta - x_0|$ is maximum. The maximum absolute error relative to the fringe width is thus

$$e \equiv \frac{|\Delta x_i|}{2\rho_i} \max = \frac{|k_d - \bar{x}|}{N} \max \quad (13)$$

where the error parameter, e , is a function of the wavemeter parameters R , SNR , Q , and N . Values of e for various values of these wavemeter

parameters are shown in the appendix. The particular value of \bar{x} which maximizes e is also shown. The values for R (0.05, 0.03, and 0.01) were chosen as somewhat representative of typical devices and employing progressive degrees of response calibration (Ref. 7). In addition to the table of values in the appendix, a plot of e vs. the number of diodes in the width, $2\rho_j$, is shown in fig. 5 for some specific wavemeter parameters. Notice that the discrete nature of the diode sampling causes fluctuations in the error parameter until the fringe width is spread over about 10 diodes.

As an example of these results an experimental situation in which $\text{SNR} = 100$, $Q = 256$, a total non-uniformity of $R = 0.05$, and $N = 10$ diodes generates a value of $e = 0.184$. The fringe center can thus be determined to about $1/5.4$ of the FWHM by the fringe peak method. If R is reduced to 0.01 by suitable calibration of the diode response and beam non-uniformities are negligible this method can determine the fringe center to approximate one-tenth of the fringe width.

Wavelength Error

The results of the preceding analysis estimate the errors, $|\Delta x_j|$, that one might expect in locating the various fringe centers by using the fringe peak method. In order to translate these results into wavelength errors through use of eq. (3), we proceed with some statistical notions regarding these coordinate errors.

As can be seen from fig. 1, the errors, ΔL and ΔX_0 , present in eq. (3) are related to the errors in the fringe locations, Δx_j , by $\Delta L = \Delta(x_u - x_0)$ and $\Delta X_0 = \Delta(x_{0+1} - x_0)$. If the fringes to be measured are spread across a large number of diodes, then repeated measurements of Δx_j would result in a histogram or probability density function, $p(\Delta x_j)$, which increases

monotonically toward the origin, i.e., it would be peaked at $\Delta x_i = 0$. A more conservative situation for these measurements would be to consider the errors as random. The probability density function would be a rectangular distribution where $p(\Delta x_i) = 0$ when $|\Delta x_i| > e(2\rho_i)$ and $p(\Delta x_i) = 1/e(2\rho_i)$ when $|\Delta x_i| \leq e(2\rho_i)$. This distribution might be reasonable when the number of diodes in the FWHM is relatively small and for situations where no a priori knowledge of the fringe location is assumed. For such a distribution, the mean square value of Δx_i is given by the expected value of $(\Delta x_i)^2$, i.e.,

$$\begin{aligned} E[(\Delta x_i)^2] &= \int_{-\infty}^{\infty} (\Delta x_i)^2 p(\Delta x_i) d(\Delta x_i) \\ &= \frac{1}{4e\rho_i} \int_{-2e\rho_i}^{2e\rho_i} (\Delta x_i)^2 d(\Delta x_i) = \left(\frac{2e\rho_i}{\sqrt{3}} \right)^2. \end{aligned} \quad (14)$$

The mean-square error obtained in eq. (14) can now be used with eq. (3) to find the mean-square error of $\Delta\lambda_u/\lambda_u$. Assuming that the coordinate error, Δx_u , is independent of the errors, Δx_0 and Δx_{0+1} , but that some correlation exists between the various orders of the known laser, an upper bound on the rms error of $\Delta\lambda_u/\lambda_u$ can be shown to be

$$\left| \frac{\Delta\lambda_u}{\lambda_u} \right|_{\text{rms}} \leq \frac{e}{\sqrt{3} m_0 \lambda_0} \left[(2\rho_u)^2 + 5(2\rho_0)^2 \right]^{1/2} \quad (15)$$

The widths, $2\rho_u$ and $2\rho_0$, in this equation are the spatial FWHM values. They can be converted to spectral FWHM values, $\delta\lambda_u$ and $\delta\lambda_0$, by

the Fizeau relationships which relate the free-spectral-range, order number, and spatial period of the fringes at the respective wavelengths, λ_u and λ_0 . If the wavelength of the standard or reference laser is chosen sufficiently close to the unknown laser wavelength, then eq. (15) becomes

$$|\Delta\lambda_u|_{\text{rms}} \leq \frac{e}{\sqrt{3}} [5(\delta\lambda_0)^2 + (\delta\lambda_u)^2]^{1/2}. \quad (16)$$

The spectral widths in the previous equation contain both the laser linewidths of the reference and unknown laser and also the resolution width of the wavemeter. If we assume that reference laser linewidth is small compared to the resolution width, and that the fringe shapes are Lorentzian, then the absolute rms error is

$$|\Delta\lambda_u|_{\text{rms}} \leq \frac{e}{\sqrt{3}} [5(\delta\lambda_R)^2 + (\delta\lambda_R + \delta\lambda_{\lambda u})^2]^{1/2} \quad (17)$$

where $\delta\lambda_R$ is the Fizeau resolution and $\delta\lambda_{\lambda u}$ is linewidth of the unknown laser. Thus, for specific values of $|\Delta\lambda_u|_{\text{rms}}$, $\delta\lambda_R$, and $\delta\lambda_{\lambda u}$, the required value of e can be determined and the corresponding values of the parameters R , SNR , Q , and N found.

Figure 6 shows an application of eq. (17) in which $|\Delta\lambda_u|_{\text{rms}}$ is plotted against the error parameter, e , for a laser linewidth of 1.0 pm and three values of wavemeter resolution. For the case of an experiment which requires absolute knowledge of the wavelength to within 0.25 pm and a resolution of 0.50 pm, eq. (17), and fig. 6, indicate that fringe locations must be determined to within 0.231 of their respective widths. From the

appendix, this value can be obtained by several combinations of the various parameters. One such combination which satisfies this value is for a sensor where the total non-uniformity of the array and input illumination has value the of $R = 0.05$, and the maximum current from the fringe is digitized by an 8-bit analog-to-digital converter ($Q = 256$). For these conditions, the value of $e = 0.231$ can be obtained if $SNR \geq 26$, and the fringe is spread over at least 10 diodes. From fig. 5, any combination of these parameters which results in the curve lying below the value of $e = 0.231$ will achieve the wavelength accuracy required in this example.

Estimate of Linecenter Using Two-Sensor Position Average

The centers of the fringes which are used to determine the wavelength can be found from procedures other than the peak method just described. One method which can be used involves searching the array for two diodes (k_d^+ and k_d^-) whose output currents are equal to within a specified tolerance. The linecenter, x_c , is then given by the average position of these two diodes, i.e., $x_c = (k_d^+ + k_d^-)\Delta/2$.

Analysis of this method for errors in determining the fringe center can begin with reference to fig. 3 where the current output from an error-free diode array is shown. For the two cases where $x_0 = 0$ and $x_0 = 0.50\Delta$, the position average of various diode pairs having equal currents gives a fringe center location which corresponds exactly with the true fringe center ($x_c = x_0$). For $x_0 = 0.25\Delta$ (or any other value between 0 and 0.50Δ) no two diodes have equal current outputs and clearly some current interval, or tolerance must be specified.

The value of this current interval is somewhat arbitrary but clearly the smallest interval that could be chosen is the quantization interval,

I_0/Q , described previously. For actual cases where noise and error sources are introduced into the fringes, searching for two diodes whose current difference is this small could lead to difficulty. One value of a specified current difference which could be used is the relative difference between two successive diodes in the FWHM region of the array output. For $x_0 = 0$ and for a perfectly uniform array response ($R=0$), this relative current interval can be shown to be given approximately by $1/N$ where N is the number of diodes contained in the FWHM.

To determine a worst-case error for finding the fringe center we proceed in a manner similar to that used in the fringe peak method. We are searching for two currents at diode locations $x_d^+ = k_d^+ \Delta$ and $x_d^- = k_d^- \Delta$ whose outputs due to both the irradiance incident on the array and all the various noise sources are equal to within some margin, δI_m . With reference to fig. 7, the current output from the array, $I_d'(k \Delta)$ (see eq. (10)), is shown plotted for an error-free system having a fringe center at $x_0 = 0$. If the various errors which were discussed in the previous analysis are now introduced into the system, a worst-case error exists by the relationship

$$I_d'(k_d^+; x_0) - \delta I_d^+ - \delta I_m = I_d'(k_d^-; x_0) + \delta I_d^- \quad (18)$$

where

$$\delta I_d^+ = I_d'(k_d^+ \Delta; x_0) - [I_d'(k_d^+; x_0, -R) - \sigma_N - \Delta I/2] \quad (19)$$

$$\delta I_d^- = [I_d'(k_d^- \Delta; x_0, R) + \sigma_N + \Delta I/2] - I_d'(k_d^- \Delta; x_0)$$

Substituting eq. (7) for I_d' , equations (18) and (19) combine to give a worst-case error condition

$$\begin{aligned} & \tan^{-1} \left[\frac{2/N}{1 + \left(\frac{k_d^+ \Delta - x_0}{\rho} \right)^2 - \frac{1}{N^2}} \right] - \tan^{-1} \left[\frac{2/N}{1 + \left(\frac{k_d^- \Delta - x_0}{\rho} \right)^2 - \frac{1}{N^2}} \right] \\ & -R \left\{ \tan^{-1} \left[\frac{2/N}{1 + \left(\frac{k_d^+ \Delta - x_0}{\rho} \right)^2 - \frac{1}{N^2}} \right] + \tan^{-1} \left[\frac{2/N}{1 + \left(\frac{k_d^- \Delta - x_0}{\rho} \right)^2 - \frac{1}{N^2}} \right] \right\} \\ & = 2 \tan^{-1} \left(\frac{1}{N} \right) \left[\frac{2\sigma_N}{I_0} + \frac{\Delta I}{I_0} + \frac{\delta I_M}{I_0} \right] . \quad (20) \end{aligned}$$

The average location of these two diodes at x_d^+ and x_d^- is given by $x_c = (k_d^+ + k_d^-) \Delta / 2$ resulting in an absolute error of the fringe linecenter of $|x_0 - x_c|$. If this absolute error relative to the width, 2ρ , is defined as in eq. (13), then one can show the following relationships:

$$e \equiv \frac{|X_o - X_c|}{2\rho}$$

$$\frac{k_d^+ \Delta - X_o}{\rho} = z - 2e \quad (21)$$

$$\frac{k_d^- \Delta - X_o}{\rho} = -z - 2e$$

where we have defined the parameter, z , by $z = (k_d^+ - k_d^-)/N$. With these equations, one may solve eq. (21) for the error parameter, e ,

$$e = \frac{(1+z^2)^2}{8z} \left[\frac{2}{\text{SNR}} + \frac{1}{Q} + \frac{\delta I_M}{I_o} \right] + \left(\frac{1+z^2}{4z} \right) R \quad (22)$$

where we have assumed $N \gg 1$ and $e/z \ll 1$.

Specific Cases

The error parameter, e , for this method of determining the fringe center can be compared to some values obtained with the fringe-peak method. If we assume the current interval, $\delta I_M/I_o$, is given by $1/N$ as discussed previously and the two sampled diodes (k_d^+ and k_d^-) are at approximately the FWHM points, then $z \approx 1$, and eq. (23) becomes

$$e(z=1) = 1/2(R + 2/\text{SNR} + 1/Q + 1/N). \quad (23)$$

For $Q = 256$ and $R = 0.05$, we have the following table of values of $e(z=1)$ vs. SNR:

Error Parameter vs. SNR and N

SNR	$e(z=1)$			
	N = 10	N = 20	N = 30	N = 40
5	0.28	0.25	0.24	0.24
10	0.18	0.15	0.14	0.14
20	0.13	0.10	0.094	0.089
30	0.11	0.085	0.077	0.073
50	0.097	0.072	0.064	0.059
75	0.090	0.065	0.057	0.053
100	0.087	0.062	0.054	0.049

Comparison of the results in this table against the corresponding values shown in the appendix for the fringe-peak method shows a smaller error. For example, for $N = 10$, $Q = 256$, $R = 0.05$, and $SNR = 100$, the fringe peak method was shown to give a value of $e = 0.184$ whereas this method gives $e = 0.087$ or a decrease of about a factor of two in the error parameter. However, it must be remembered that we have applied this two-position sensor average procedure to relatively smooth fringe shapes. In many cases, especially those where the wavelength of pulsed, multi-mode lasers is to be determined, the shapes are more complex and often have multiple, asymmetric peaks. In addition, the pulse-to-pulse repeatability of these complex shapes have not been characterized sufficiently for inclusion in this error analysis. For these reasons, then, one would expect that the improved accuracy shown in the latter method would decrease and approach that obtained by measuring only the peaks. It may be possible, however, to regain some of this accuracy by using more than one pair of pixel outputs in a statistical averaging process.

Conclusions

The wavelength accuracy that can be obtained from wavemeters employing multiple-beam Fizeau interferometers and CCD-type readouts is dependent upon several parameters. The non-uniformity of the detector array response and fluctuations found in the wavemeter input illumination affect the accuracy as well as the current fluctuations in the output due to noise sources such as current quantization errors and electronic signal-to-noise ratio. Since the wavelength is determined by measuring the locations of fringe sets generated by the wavemeter, the method used to determine the fringe coordinates also affects the accuracy. The two procedures investigated in this paper showed that greater accuracy can be obtained on smooth, repeatable laser pulses by the two-position sensor average method, but that a simpler technique exists in which only the peak locations are measured. Furthermore, when complex, non-repeatable fringe shapes are included, the accuracies of the two methods are similar unless a statistical averaging process is applied to more than one sensor-pair.

References

1. Morris, M. B., McIlrath, T. J., Snyder, J. J., Fizeau Wavemeter for Pulsed Laser Wavelength Measurement, *Applied Optics* 23, 3862 (1984).
2. Morris, M. B., McIlrath, T. J., Portable High-Resolution Monochrometer-Interferometer with Multichannel Electronic Readout, *Applied Optics* 18, 4145 (1979).
3. Bennett, K., Byer, R. L., 30-MHz Resolution Digital Wavelength Meter for Pulsed or CW Lasers, *J.O.S.A.* 70, 1566 (1980).
4. Rogers, J. R., Fringe Shifts in Multiple-Beam Fizeau Interferometry, *J.O.S.A.* 72, 638 (1982).
5. Kinoshita, K., Numerical Evaluation of the Intensity Curve of a Multiple-Beam Fizeau Fringe, *J. Physical Soc. of Japan* 8, 219 (1953).
6. Steel, W. H., *Interferometry* (2nd Edition), Cambridge University Press, New York, (1983), p. 149.
7. Tanaka, S. C., A Need and Method for Nonuniformity Correction in Solid State Image Sensors, S.P.I.E. Conference on Focal Plane Methodologies III, Aug. 24-25, 1982, San Diego, CA.

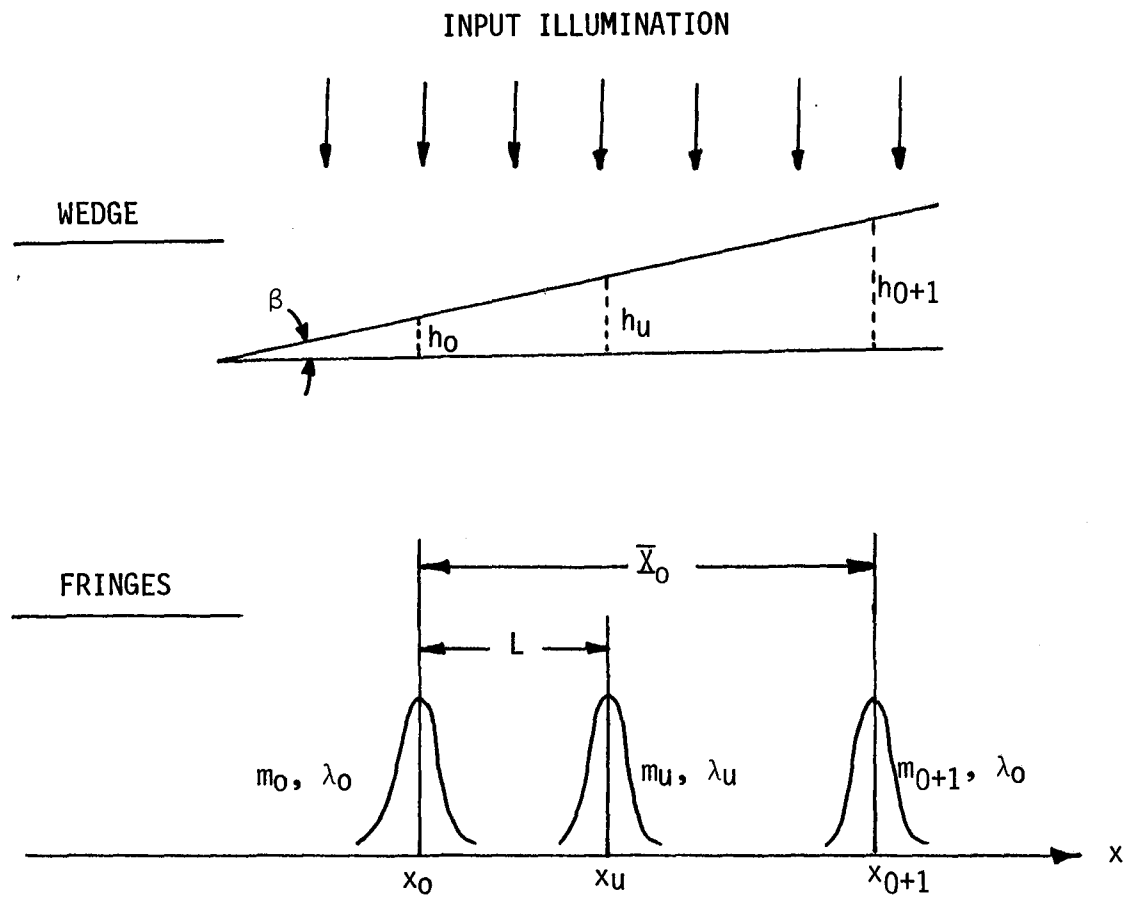


Figure 1.- Fizeau wedge geometry and output fringe location.

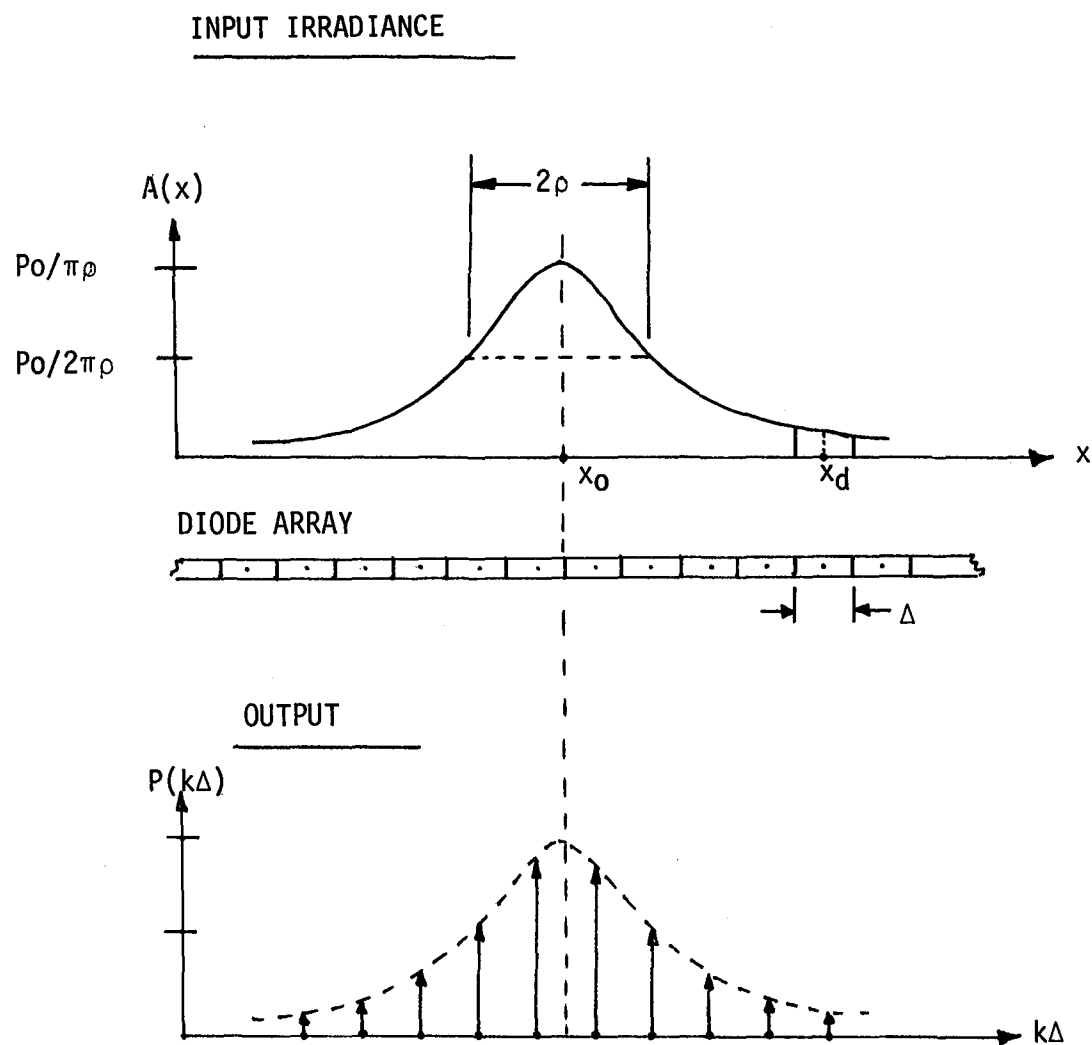


Figure 2.- Single fringe irradiance and corresponding optical power incident on the diode elements.

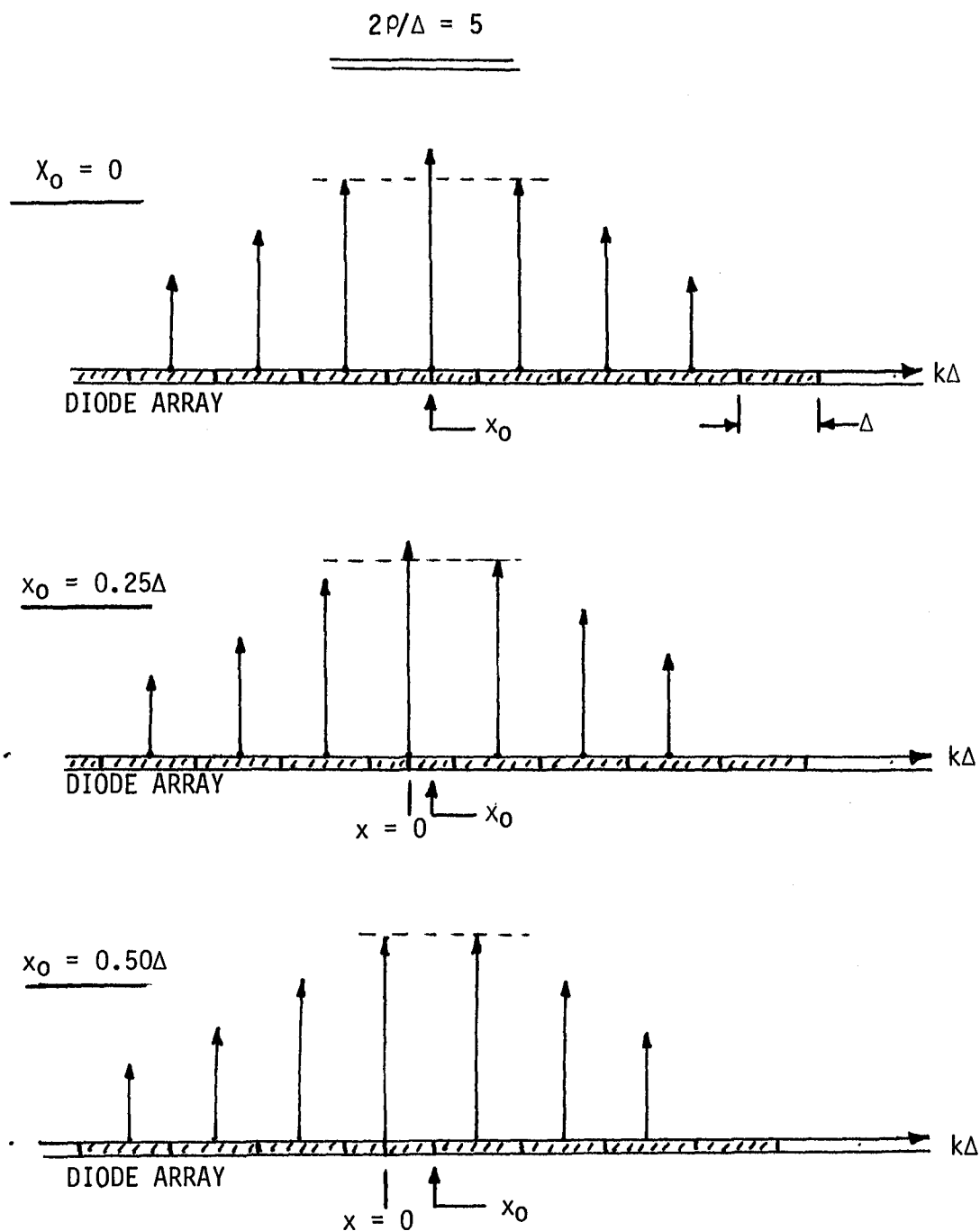


Figure 3.- Normalized output current for uniform response and different values of x_0 .

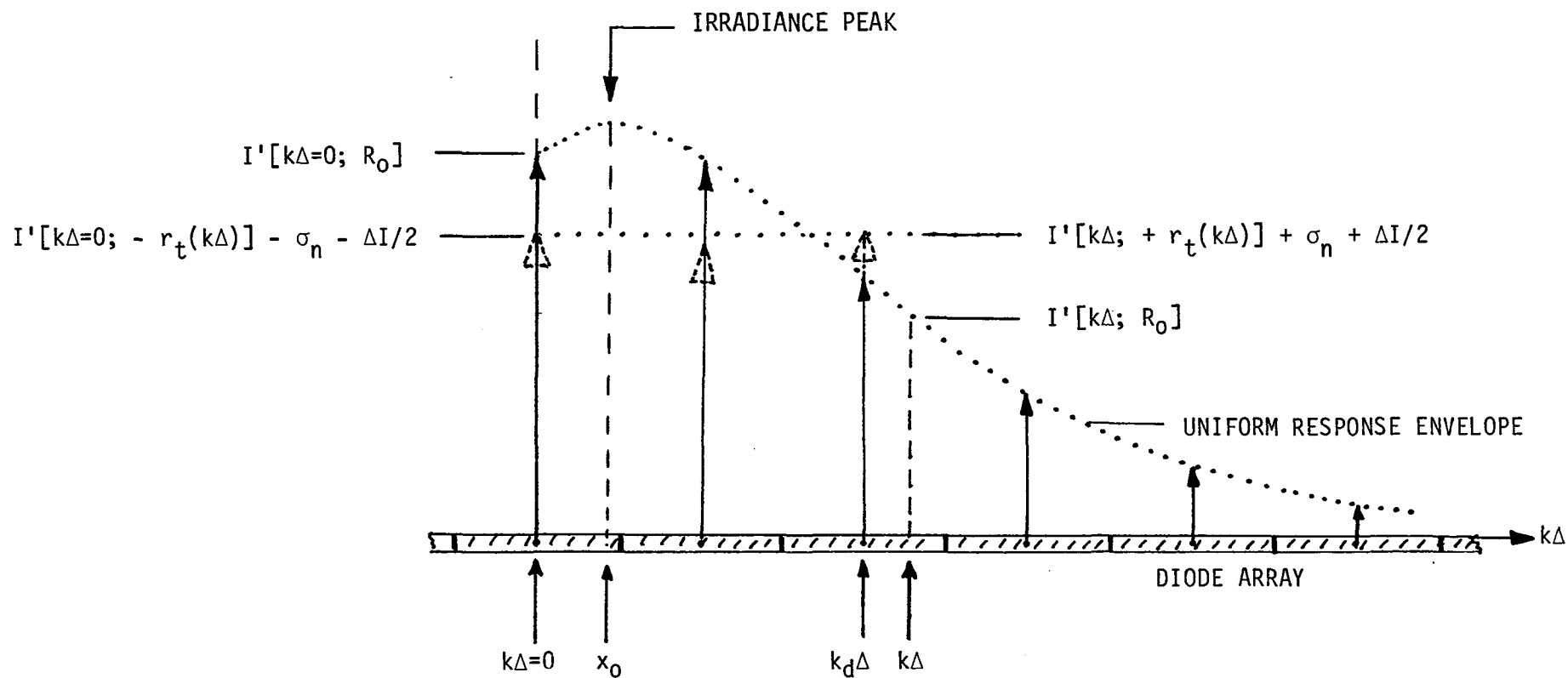


Figure 4.- Error in true peak location due to current fluctuations.
Actual location of x_0 is unknown to $\pm 0.50\Delta$.

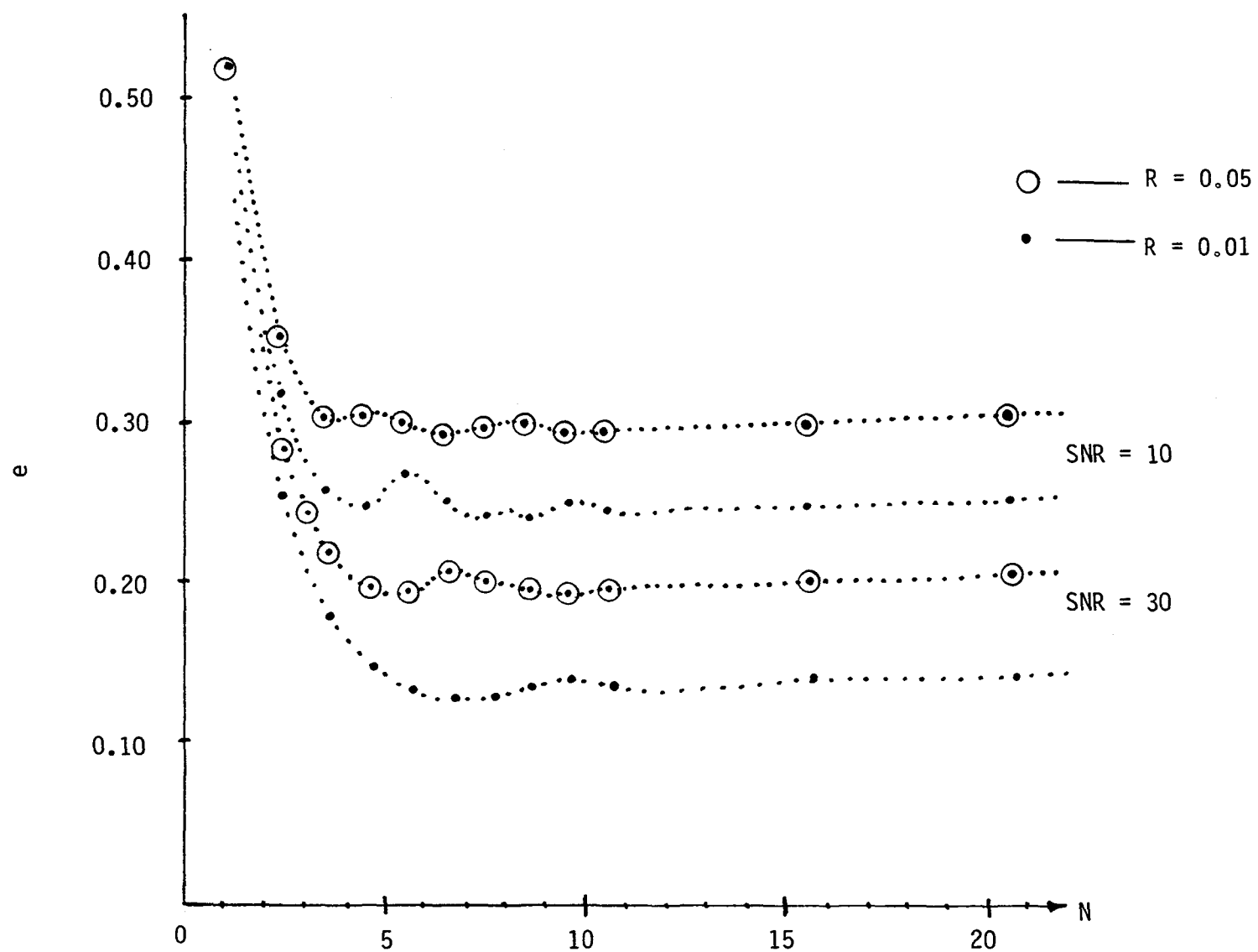


Figure 5.- Error parameter vs. number of diodes in fringe width.

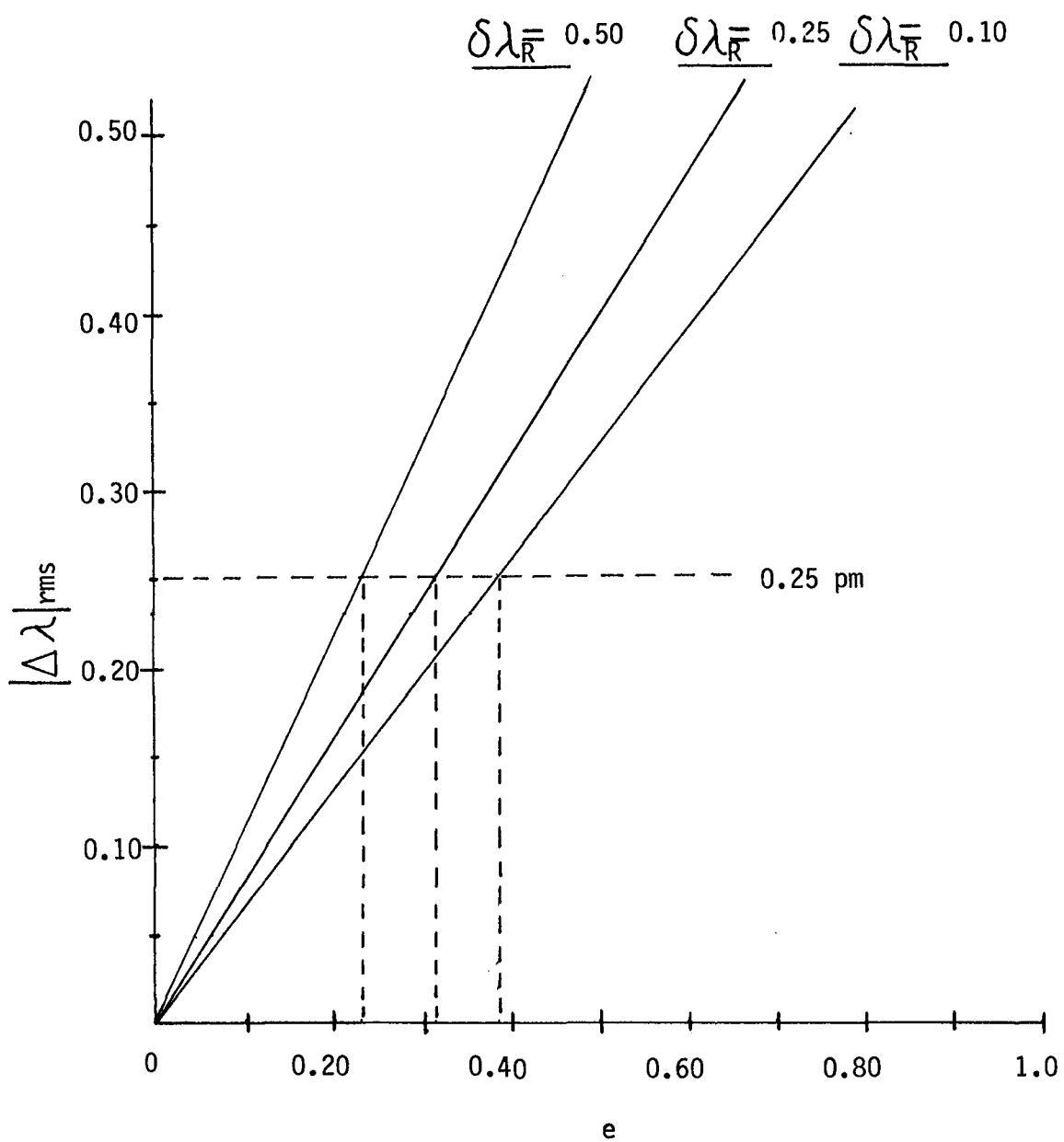


Figure 6.- Absolute wavelength error vs. error parameter for three values of resolution.

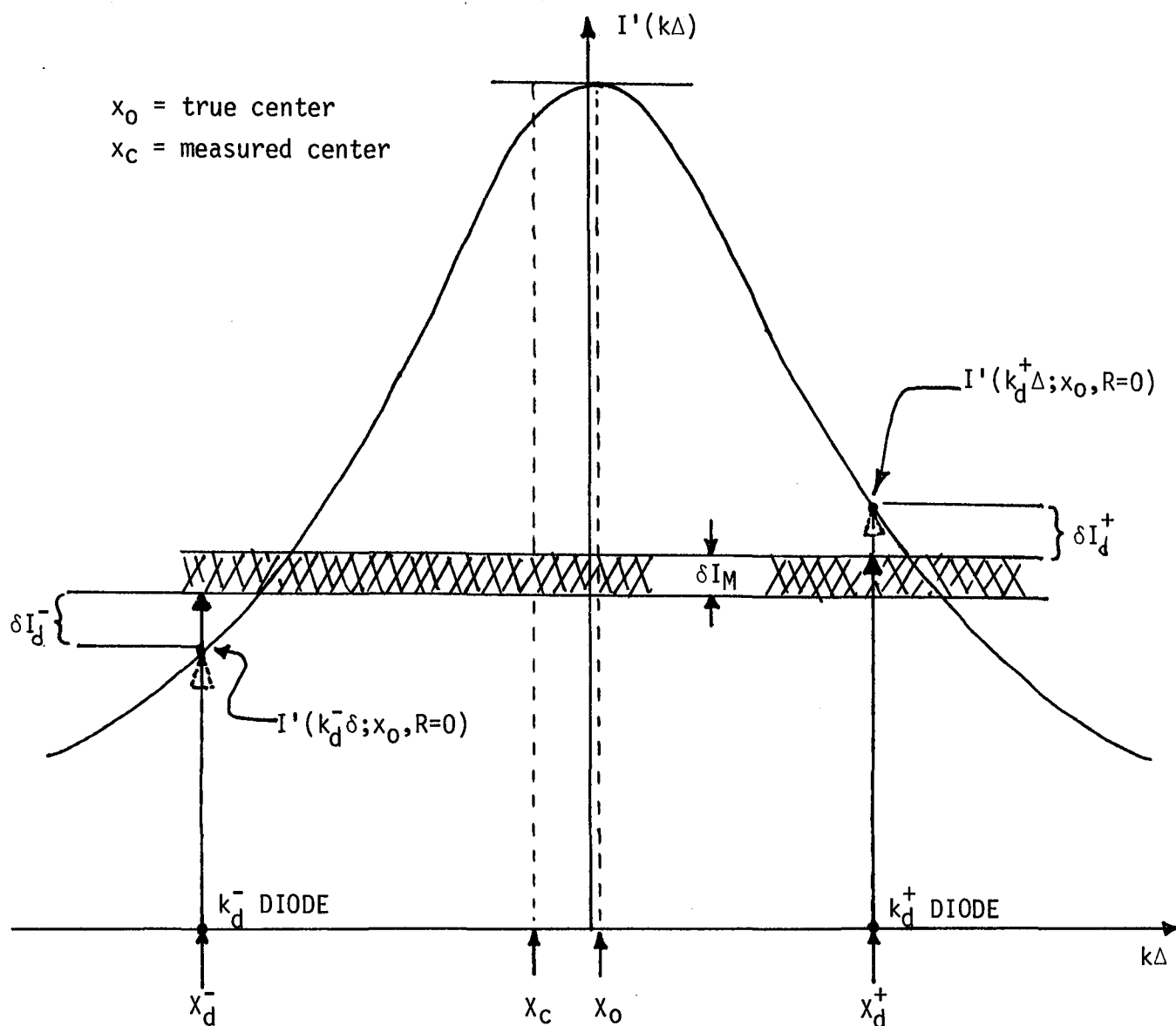


Figure 7.- Geometry for estimating fringe center using two-sensor position average.

Error Parameter vs. System Parameters					
e	\bar{X}	R	Q	SNR	N
1.27000	.4600	.050	256	3	2
1.25500	.4900	.030	256	3	2
.87500	.2500	.010	256	3	2
1.27000	.4600	.050	512	3	2
1.25000	-.5000	.030	512	3	2
1.25000	.5000	.030	512	3	2
.87000	.2600	.010	512	3	2
.39000	.2200	.050	256	10	2
.37000	.2600	.030	256	10	2
.35500	.2900	.010	256	10	2
.39000	.2200	.050	512	10	2
.37000	.2600	.030	512	10	2
.35500	.2900	.010	512	10	2
.30000	.4000	.050	256	100	2
.28000	.4400	.030	256	100	2
.26500	.4700	.010	256	100	2
.29500	.4100	.050	512	100	2
.28000	.4400	.030	512	100	2
.26500	.4700	.010	512	100	2
.29000	.4200	.050	256	300	2
.27500	.4500	.030	256	300	2
.26000	.4800	.010	256	300	2
.29000	.4200	.050	512	300	2
.27500	.4500	.030	512	300	2
.26000	.4800	.010	512	300	2
.29000	.4200	.050	256	1000	2
.27500	.4500	.030	256	1000	2
.26000	.4800	.010	256	1000	2
.29000	.4200	.050	512	1000	2
.27500	.4500	.030	512	1000	2
.25500	.4900	.010	512	1000	2

e	\bar{X}	R	Q	SNR	N
.91000	.2700	.050	256	3	3
.88667	.3400	.030	256	3	3
.86667	.4000	.010	256	3	3
.91000	.2700	.050	512	3	3
.88667	.3400	.030	512	3	3
.86667	.4000	.010	512	3	3
.34000	-.0200	.050	256	10	3
.31333	.0600	.030	256	10	3
.29000	.1300	.010	256	10	3
.33667	-.0100	.050	512	10	3
.31333	.0600	.030	512	10	3
.29000	.1300	.010	512	10	3
.22667	.3200	.050	256	100	3
.20667	.3800	.030	256	100	3
.18667	.4400	.010	256	100	3
.22333	.3300	.050	512	100	3
.20667	.3800	.030	512	100	3
.18667	.4400	.010	512	100	3
.22000	.3400	.050	256	300	3
.20000	.4000	.030	256	300	3
.18000	.4600	.010	256	300	3
.21667	.3500	.050	512	300	3
.19667	.4100	.030	512	300	3
.18000	.4600	.010	512	300	3
.21667	.3500	.050	256	1000	3
.19667	.4100	.030	256	1000	3
.17667	.4700	.010	256	1000	3
.21667	.3500	.050	512	1000	3
.19667	.4100	.030	512	1000	3
.17667	.4700	.010	512	1000	3

e	\bar{X}	R	Q	SNR	N
.90750	.3700	.050	256	3	4
.88500	.4600	.030	256	3	4
.75000	0.0000	.010	256	3	4
.90500	.3800	.050	512	3	4
.88250	.4700	.030	512	3	4
.74750	.0100	.010	512	3	4
.36250	-.4500	.050	256	10	4
.31750	-.2700	.030	256	10	4
.28000	-.1200	.010	256	10	4
.36000	-.4400	.050	512	10	4
.31500	-.2600	.030	512	10	4
.27750	-.1100	.010	512	10	4
.19750	.2100	.050	256	100	4
.17250	.3100	.030	256	100	4
.15000	.4000	.010	256	100	4
.19750	.2100	.050	512	100	4
.17250	.3100	.030	512	100	4
.15000	.4000	.010	512	100	4
.19000	.2400	.050	256	300	4
.16500	.3400	.030	256	300	4
.14250	.4300	.010	256	300	4
.18750	.2500	.050	512	300	4
.16500	.3400	.030	512	300	4
.14000	.4400	.010	512	300	4
.18500	.2600	.050	256	1000	4
.16250	.3500	.030	256	1000	4
.14000	.4400	.010	256	1000	4
.18500	.2600	.050	512	1000	4
.16000	.3600	.030	512	1000	4
.13750	.4500	.010	512	1000	4

e	\bar{X}	R	Q	SNR	N
.90600	.4700	.050	256	3	5
.79200	.0400	.030	256	3	5
.75600	.2200	.010	256	3	5
.90400	.4800	.050	512	3	5
.78800	.0600	.030	512	3	5
.75400	.2300	.010	512	3	5
.33600	.3200	.050	256	10	5
.31800	.4100	.030	256	10	5
.30000	-.5000	.010	256	10	5
.30000	.5000	.010	256	10	5
.33600	.3200	.050	512	10	5
.31600	.4200	.030	512	10	5
.30000	-.5000	.010	512	10	5
.30000	.5000	.010	512	10	5
.18800	.0600	.050	256	100	5
.15800	.2100	.030	256	100	5
.13000	.3500	.010	256	100	5
.18600	.0700	.050	512	100	5
.15600	.2200	.030	512	100	5
.12800	.3600	.010	512	100	5
.17800	.1100	.050	256	300	5
.14800	.2600	.030	256	300	5
.12000	.4000	.010	256	300	5
.17600	.1200	.050	512	300	5
.14600	.2700	.030	512	300	5
.11800	.4100	.010	512	300	5
.17400	.1300	.050	256	1000	5
.14400	.2800	.030	256	1000	5
.11800	.4100	.010	256	1000	5
.17200	.1400	.050	512	1000	5
.14400	.2800	.030	512	1000	5
.11600	.4200	.010	512	1000	5

e	\bar{X}	R	Q	SNR	N
.83833	-.0300	.050	256	3	6
.79667	.2200	.030	256	3	6
.76833	.3900	.010	256	3	6
.83333	0.0000	.050	512	3	6
.79500	.2300	.030	512	3	6
.76667	.4000	.010	512	3	6
.32333	.0600	.050	256	10	6
.30000	.2000	.030	256	10	6
.28000	.3200	.010	256	10	6
.32333	.0600	.050	512	10	6
.30000	.2000	.030	512	10	6
.27833	.3300	.010	512	10	6
.18667	-.1200	.050	256	100	6
.15167	.0900	.030	256	100	6
.11833	.2900	.010	256	100	6
.18500	-.1100	.050	512	100	6
.15000	.1000	.030	512	100	6
.11667	.3000	.010	512	100	6
.17500	-.0500	.050	256	300	6
.14000	.1600	.030	256	300	6
.10667	.3600	.010	256	300	6
.17333	-.0400	.050	512	300	6
.13833	.1700	.030	512	300	6
.10500	.3700	.010	512	300	6
.17000	-.0200	.050	256	1000	6
.13667	.1800	.030	256	1000	6
.10333	.3800	.010	256	1000	6
.16833	-.0100	.050	512	1000	6
.13500	.1900	.030	512	1000	6
.10167	.3900	.010	512	1000	6

e	\bar{X}	R	Q	SNR	N
.83857	.1300	.050	256	3	7
.80429	.3700	.030	256	3	7
.74714	-.2300	.010	256	3	7
.83429	.1600	.050	512	3	7
.80286	.3800	.030	512	3	7
.74143	-.1900	.010	512	3	7
.32714	-.2900	.050	256	10	7
.29714	-.0800	.030	256	10	7
.27000	.1100	.010	256	10	7
.32571	-.2800	.050	512	10	7
.29571	-.0700	.030	512	10	7
.26857	.1200	.010	512	10	7
.19286	-.3500	.050	256	100	7
.15143	-.0600	.030	256	100	7
.11143	.2200	.010	256	100	7
.19000	-.3300	.050	512	100	7
.14857	-.0400	.030	512	100	7
.11000	.2300	.010	512	100	7
.17714	-.2400	.050	256	300	7
.13714	.0400	.030	256	300	7
.09857	.3100	.010	256	300	7
.17571	-.2300	.050	512	300	7
.13571	.0500	.030	512	300	7
.09714	.3200	.010	512	300	7
.17286	-.2100	.050	256	1000	7
.13286	.0700	.030	256	1000	7
.09429	.3400	.010	256	1000	7
.17000	-.1900	.050	512	1000	7
.13000	.0900	.030	512	1000	7
.09286	.3500	.010	512	1000	7

e	\bar{X}	R	Q	SNR	N
.84250	.2600	.050	256	3	8
.81250	-.5000	.030	256	3	8
.81250	.5000	.030	256	3	8
.74000	.0800	.010	256	3	8
.83875	.2900	.050	512	3	8
.79750	-.3800	.030	512	3	8
.73625	.1100	.010	512	3	8
.32750	.3800	.050	256	10	8
.30500	-.4400	.030	256	10	8
.27000	-.1600	.010	256	10	8
.32625	.3900	.050	512	10	8
.30250	-.4200	.030	512	10	8
.26875	-.1500	.010	512	10	8
.19375	.4500	.050	256	100	8
.15250	-.2200	.030	256	100	8
.10875	.1300	.010	256	100	8
.19250	.4600	.050	512	100	8
.15125	-.2100	.030	512	100	8
.10625	.1500	.010	512	100	8
.18375	-.4700	.050	256	300	8
.13750	-.1000	.030	256	300	8
.09375	.2500	.010	256	300	8
.18125	-.4500	.050	512	300	8
.13500	-.0800	.030	512	300	8
.09250	.2600	.010	512	300	8
.17750	-.4200	.050	256	1000	8
.13250	-.0600	.030	256	1000	8
.08875	.2900	.010	256	1000	8
.17500	-.4000	.050	512	1000	8
.13000	-.0400	.030	512	1000	8
.08750	.3000	.010	512	1000	8

e	\bar{X}	R	Q	SNR	N
.84667	.3800	.050	256	3	9
.78444	-.0600	.030	256	3	9
.74444	.3000	.010	256	3	9
.84444	.4000	.050	512	3	9
.78000	-.0200	.030	512	3	9
.74222	.3200	.010	512	3	9
.32111	.1100	.050	256	10	9
.29889	.3100	.030	256	10	9
.27778	-.5000	.010	256	10	9
.27778	.5000	.010	256	10	9
.32000	.1200	.050	512	10	9
.29778	.3200	.030	512	10	9
.27556	-.4800	.010	512	10	9
.18778	.3100	.050	256	100	9
.15778	-.4200	.030	256	100	9
.10667	.0400	.010	256	100	9
.18667	.3200	.050	512	100	9
.15556	-.4000	.030	512	100	9
.10444	.0600	.010	512	100	9
.17889	.3900	.050	256	300	9
.14000	-.2600	.030	256	300	9
.09111	.1800	.010	256	300	9
.17778	.4000	.050	512	300	9
.13667	-.2300	.030	512	300	9
.08889	.2000	.010	512	300	9
.17556	.4200	.050	256	1000	9
.13333	-.2000	.030	256	1000	9
.08556	.2300	.010	256	1000	9
.17444	.4300	.050	512	1000	9
.13111	-.1800	.030	512	1000	9
.08333	.2500	.010	512	1000	9

e	\bar{X}	R	Q	SNR	N
.85100	.4900	.050	256	3	10
.78500	.1500	.030	256	3	10
.75200	.4800	.010	256	3	10
.84300	-.4300	.050	512	3	10
.78200	.1800	.030	512	3	10
.75000	-.5000	.010	512	3	10
.75000	.5000	.010	512	3	10
.32200	-.2200	.050	256	10	10
.29500	.0500	.030	256	10	10
.27100	.2900	.010	256	10	10
.32000	-.2000	.050	512	10	10
.29400	.0600	.030	512	10	10
.26900	.3100	.010	512	10	10
.18400	.1600	.050	256	100	10
.15600	.4400	.030	256	100	10
.10700	-.0700	.010	256	100	10
.18300	.1700	.050	512	100	10
.15500	.4500	.030	512	100	10
.10500	-.0500	.010	512	100	10
.17400	.2600	.050	256	300	10
.14400	-.4400	.030	256	300	10
.08900	.1100	.010	256	300	10
.17300	.2700	.050	512	300	10
.14100	-.4100	.030	512	300	10
.08700	.1300	.010	512	300	10
.17100	.2900	.050	256	1000	10
.13700	-.3700	.030	256	1000	10
.08300	.1700	.010	256	1000	10
.16900	.3100	.050	512	1000	10
.13400	-.3400	.030	512	1000	10
.08000	.2000	.010	512	1000	10

e	\bar{X}	R	Q	SNR	N
.83733	.4400	.050	256	3	15
.78400	.2400	.030	256	3	15
.73600	-.0400	.010	256	3	15
.83467	.4800	.050	512	3	15
.78067	.2900	.030	512	3	15
.73267	.0100	.010	512	3	15
.32000	.2000	.050	256	10	15
.29667	-.4500	.030	256	10	15
.26733	-.0100	.010	256	10	15
.31867	.2200	.050	512	10	15
.29467	-.4200	.030	512	10	15
.26600	.0100	.010	512	10	15
.18400	.2400	.050	256	100	15
.15000	-.2500	.030	256	100	15
.10933	.3600	.010	256	100	15
.18267	.2600	.050	512	100	15
.14800	-.2200	.030	512	100	15
.10733	.3900	.010	512	100	15
.17400	.3900	.050	256	300	15
.13600	-.0400	.030	256	300	15
.09200	-.3800	.010	256	300	15
.17267	.4100	.050	512	300	15
.13400	-.0100	.030	512	300	15
.08800	-.3200	.010	512	300	15
.17067	.4400	.050	256	1000	15
.13067	.0400	.030	256	1000	15
.08267	-.2400	.010	256	1000	15
.16933	.4600	.050	512	1000	15
.12867	.0700	.030	512	1000	15
.07867	-.1800	.010	512	1000	15

e	\bar{X}	R	Q	SNR	N
.83300	.3400	.050	256	3	20
.78350	.3300	.030	256	3	20
.73650	.2700	.010	256	3	20
.83000	.4000	.050	512	3	20
.78050	.3900	.030	512	3	20
.73400	.3200	.010	512	3	20
.32050	-.4100	.050	256	10	20
.29400	.1200	.030	256	10	20
.26800	-.3600	.010	256	10	20
.31900	-.3800	.050	512	10	20
.29250	.1500	.030	512	10	20
.26650	-.3300	.010	512	10	20
.18400	.3200	.050	256	100	20
.14900	.0200	.030	256	100	20
.10700	-.1400	.010	256	100	20
.18250	.3500	.050	512	100	20
.14700	.0600	.030	512	100	20
.10400	-.0800	.010	512	100	20
.17350	-.4700	.050	256	300	20
.13650	.2700	.030	256	300	20
.08900	.2200	.010	256	300	20
.17150	-.4300	.050	512	300	20
.13450	.3100	.030	512	300	20
.08650	.2700	.010	512	300	20
.16850	-.3700	.050	256	1000	20
.13200	.3600	.030	256	1000	20
.08300	.3400	.010	256	1000	20
.16700	-.3400	.050	512	1000	20
.13000	.4000	.030	512	1000	20
.08050	.3900	.010	512	1000	20

e	\bar{X}	R	Q	SNR	N
.83120	.2200	.050	256	3	25
.78320	.4200	.030	256	3	25
.73760	-.4400	.010	256	3	25
.82760	.3100	.050	512	3	25
.78040	.4900	.030	512	3	25
.73320	-.3300	.010	512	3	25
.31920	.0200	.050	256	10	25
.29400	-.3500	.030	256	10	25
.26760	.3100	.010	256	10	25
.31800	.0500	.050	512	10	25
.29240	-.3100	.030	512	10	25
.26600	.3500	.010	512	10	25
.18360	.4100	.050	256	100	25
.14920	.2700	.030	256	100	25
.10720	.3200	.010	256	100	25
.18240	.4400	.050	512	100	25
.14760	.3100	.030	512	100	25
.10520	.3700	.010	512	100	25
.17200	-.3000	.050	256	300	25
.13680	-.4200	.030	256	300	25
.08880	-.2200	.010	256	300	25
.17040	-.2600	.050	512	300	25
.13440	-.3600	.030	512	300	25
.08560	-.1400	.010	512	300	25
.16760	-.1900	.050	256	1000	25
.13120	-.2800	.030	256	1000	25
.08120	-.0300	.010	256	1000	25
.16600	-.1500	.050	512	1000	25
.12880	-.2200	.030	512	1000	25
.07800	.0500	.010	512	1000	25

e	\bar{X}	R	Q	SNR	N
.83067	.0800	.050	256	3	30
.78300	-.4900	.030	256	3	30
.73533	-.0600	.010	256	3	30
.82700	.1900	.050	512	3	30
.77867	-.3600	.030	512	3	30
.73200	.0400	.010	512	3	30
.31967	.4100	.050	256	10	30
.29367	.1900	.030	256	10	30
.26700	-.0100	.010	256	10	30
.31833	.4500	.050	512	10	30
.29233	.2300	.030	512	10	30
.26533	.0400	.010	512	10	30
.18367	.4900	.050	256	100	30
.15000	-.5000	.030	256	100	30
.15000	.5000	.030	256	100	30
.10667	-.2000	.010	256	100	30
.18200	-.4600	.050	512	100	30
.14767	-.4300	.030	512	100	30
.10400	-.1200	.010	512	100	30
.17167	-.1500	.050	256	300	30
.13567	-.0700	.030	256	300	30
.08900	.3300	.010	256	300	30
.17000	-.1000	.050	512	300	30
.13367	-.0100	.030	512	300	30
.08633	.4100	.010	512	300	30
.16733	-.0200	.050	256	1000	30
.13067	.0800	.030	256	1000	30
.08267	-.4800	.010	256	1000	30
.16567	.0300	.050	512	1000	30
.12867	.1400	.030	512	1000	30
.07867	-.3600	.010	512	1000	30

e	\bar{X}	R	Q	SNR	N
.83057	-.0700	.050	256	3	35
.78200	-.3700	.030	256	3	35
.73571	.2500	.010	256	3	35
.82657	.0700	.050	512	3	35
.77771	-.2200	.030	512	3	35
.73257	.3600	.010	512	3	35
.31914	-.1700	.050	256	10	35
.29371	-.2800	.030	256	10	35
.26714	-.3500	.010	256	10	35
.31771	-.1200	.050	512	10	35
.29229	-.2300	.030	512	10	35
.26571	-.3000	.010	512	10	35
.18343	-.4200	.050	256	100	35
.14914	-.2200	.030	256	100	35
.10686	.2600	.010	256	100	35
.18143	-.3500	.050	512	100	35
.14714	-.1500	.030	512	100	35
.10457	.3400	.010	512	100	35
.17143	0.0000	.050	256	300	35
.13571	.2500	.030	256	300	35
.08829	-.0900	.010	256	300	35
.16971	.0600	.050	512	300	35
.13371	.3200	.030	512	300	35
.08543	.0100	.010	512	300	35
.16743	.1400	.050	256	1000	35
.13114	.4100	.030	256	1000	35
.08114	.1600	.010	256	1000	35
.16571	.2000	.050	512	1000	35
.12943	.4700	.030	512	1000	35
.07829	.2600	.010	512	1000	35

e	\bar{X}	R	Q	SNR	N
.83050	-.2200	.050	256	3	40
.78125	-.2500	.030	256	3	40
.73600	-.4400	.010	256	3	40
.82650	-.0600	.050	512	3	40
.77750	-.1000	.030	512	3	40
.73225	-.2900	.010	512	3	40
.31925	.2300	.050	256	10	40
.29350	.2600	.030	256	10	40
.26700	.3200	.010	256	10	40
.31775	.2900	.050	512	10	40
.29225	.3100	.030	512	10	40
.26550	.3800	.010	512	10	40
.18300	-.3200	.050	256	100	40
.14875	.0500	.030	256	100	40
.10675	-.2700	.010	256	100	40
.18125	-.2500	.050	512	100	40
.14700	.1200	.030	512	100	40
.10400	-.1600	.010	512	100	40
.17150	.1400	.050	256	300	40
.13600	-.4400	.030	256	300	40
.08900	.4400	.010	256	300	40
.17000	.2000	.050	512	300	40
.13375	-.3500	.030	512	300	40
.08600	-.4400	.010	512	300	40
.16750	.3000	.050	256	1000	40
.13075	-.2300	.030	256	1000	40
.08125	-.2500	.010	256	1000	40
.16600	.3600	.050	512	1000	40
.12875	-.1500	.030	512	1000	40
.07800	-.1200	.010	512	1000	40

e	\bar{X}	R	Q	SNR	N
.83089	-.3900	.050	256	3	45
.78111	-.1500	.030	256	3	45
.73533	-.0900	.010	256	3	45
.82667	-.2000	.050	512	3	45
.77756	.0100	.030	512	3	45
.73200	.0600	.010	512	3	45
.31933	-.3700	.050	256	10	45
.29356	-.2100	.030	256	10	45
.26689	-.0100	.010	256	10	45
.31778	-.3000	.050	512	10	45
.29200	-.1400	.030	512	10	45
.26533	.0600	.010	512	10	45
.18289	-.2300	.050	256	100	45
.14911	.2900	.030	256	100	45
.10667	.2000	.010	256	100	45
.18133	-.1600	.050	512	100	45
.14711	.3800	.030	512	100	45
.10422	.3100	.010	512	100	45
.17156	.2800	.050	256	300	45
.13556	-.1000	.030	256	300	45
.08822	.0300	.010	256	300	45
.17000	.3500	.050	512	300	45
.13356	-.0100	.030	512	300	45
.08533	.1600	.010	512	300	45
.16778	.4500	.050	256	1000	45
.13067	.1200	.030	256	1000	45
.08133	.3400	.010	256	1000	45
.16600	-.4700	.050	512	1000	45
.12867	.2100	.030	512	1000	45
.07844	.4700	.010	512	1000	45

e	\bar{X}	R	Q	SNR	N
.83100	.4500	.050	256	3	50
.78100	-.0500	.030	256	3	50
.73540	.2300	.010	256	3	50
.82680	-.3400	.050	512	3	50
.77740	.1300	.030	512	3	50
.73220	.3900	.010	512	3	50
.31900	.0500	.050	256	10	50
.29360	.3200	.030	256	10	50
.26700	-.3500	.010	256	10	50
.31760	.1200	.050	512	10	50
.29220	.3900	.030	512	10	50
.26540	-.2700	.010	512	10	50
.18280	-.1400	.050	256	100	50
.14920	-.4600	.030	256	100	50
.10680	-.3400	.010	256	100	50
.18120	-.0600	.050	512	100	50
.14720	-.3600	.030	512	100	50
.10420	-.2100	.010	512	100	50
.17180	.4100	.050	256	300	50
.13560	.2200	.030	256	300	50
.08880	-.4400	.010	256	300	50
.17020	.4900	.050	512	300	50
.13360	.3200	.030	512	300	50
.08560	-.2800	.010	512	300	50
.16760	-.3800	.050	256	1000	50
.13100	.4500	.030	256	1000	50
.08100	-.0500	.010	256	1000	50
.16580	-.2900	.050	512	1000	50
.12900	-.4500	.030	512	1000	50
.07780	.1100	.010	512	1000	50

1. Report No. NASA TM-87614		2. Government Accession No.		3. Recipient's Catalog No.	
4. Title and Subtitle Wavelength Error Analysis in a Multiple-Beam Fizeau Laser Wavemeter Having a Linear Diode Array Readout				5. Report Date December 1985	
				6. Performing Organization Code 618-32-33-01	
7. Author(s) Don M. Robinson, Carl L. Fales, Jr., and Milton W. Skolaut, Jr.				8. Performing Organization Report No.	
				10. Work Unit No.	
9. Performing Organization Name and Address NASA Langley Research Center Hampton, Virginia 23665-5225				11. Contract or Grant No.	
				13. Type of Report and Period Covered Technical Memorandum	
12. Sponsoring Agency Name and Address National Aeronautics and Space Administration Washington, D.C. 20546				14. Sponsoring Agency Code	
15. Supplementary Notes					
16. Abstract An estimate of the wavelength accuracy of a laser wavemeter is performed for a system consisting of a multiple-beam Fizeau interferometer and a linear photosensor array readout. The analysis consists of determining the fringe position errors which result when various noise sources are included in the fringe forming and detection process. Two methods of estimating the fringe centers are considered: 1) maximum pixel current location, and 2) average pixel location for two detectors with nearly equal output currents. Wavelength error results for these two methods are compared for some typical wavemeter parameters.					
17. Key Words (Suggested by Author(s)) Wavemeter, Interferometry			18. Distribution Statement Unclassified-Unlimited Subject Category 74		
19. Security Classif. (of this report) Unclassified		20. Security Classif. (of this page) Unclassified		21. No. of Pages 45	
				22. Price A03	

